https://doi.org/10.48048/tis.2025.9047

In Silico and *In Vitro* Studies of Rutin from *Syzygium cumini* (L.) Skeels. var. *album* as an Antidiabetic α-Glucosidase Enzyme Inhibitor

Yanu Andhiarto[1,2], Sukardiman[3,*], Suciati[3], Andi Rifki Rosandy[4], Faisal Akhmal Muslikh[2] and Pramudita Riwanti[2]

[1]Doctoral Program of Pharmaceutical Sciences, Faculty of Pharmacy, Universitas Airlangga, Surabaya 60115, Indonesia
[2]Department of Pharmaceutical Sciences, Faculty of Pharmacy, Universitas Hang Tuah, Surabaya 60111, Indonesia
[3]Department of Pharmaceutical Sciences, Faculty of Pharmacy, Universitas Airlangga, Surabaya 60115, Indonesia
[4]University Center of Excellence for Nutraceuticals, Biosciences and Biotechnology Research Center, Bandung Institute of Technology, Bandung 40132, Indonesia

([*]Corresponding author's e-mail: sukardiman@ff.unair.ac.id)

Received: 20 September 2024, Revised: 16 October 2024, Accepted: 23 October 2024, Published: 10 December 2024

Abstract

Diabetes is a serious global condition, ranking among the top 10 causes of adult death. Current α-glucosidase inhibitors (AGI) have undesirable side effects, highlighting the need to develop new AGI drugs with lower side effects using medicinal plants. Java plum (*Syzygium cumini* var. *album*) have traditionally been used to lower blood sugar. This study aimed to isolate active compounds from *S. cumini* and evaluate their activity against α-glucosidase inhibition, both *in vitro* and through computational modeling. The leaves and stem bark of *S. cumini* var. *album* were extracted using 70 % ethanol, while n-hexane, ethyl acetate, butanol, and water were used as solvents in the fractionation process. The mixtures were then eluted in a gradient manner using column chromatography, and the selected fraction was further isolated by radial chromatography. Identification of the isolated compounds was carried out based on spectroscopic data. Molecular docking was conducted using AutoDockTools 4.2.6 and visualized using BIOVIA Discovery Studio Visualizer v.21.1.0.20298. The results confirmed that the isolated compound identifies it as rutin. Acarbose was used as a reference drug in this study. Based on the docking results, rutin exhibited a more negative ΔG compared to acarbose. The binding energy for these interactions was –3.17 kcal/mol. The binding properties of this α-glucosidase inhibitor resemble those of acarbose. Rutin has an IC_{50} value of 48.36 ± 0.4 μg/mL, which is slightly higher than that of acarbose, at 45.84 ± 0.27 μg/mL, in inhibiting α-glucosidase. Overall, rutin isolated from *S. cumini* var. *album* leaves shows potential for development as an anti-diabetic drug by inhibiting α-glucosidase.

Keywords: Rutin, *Syzygium cumini*, α-glucosidase, Diabetes mellitus (DM)

Introduction

Diabetes is a serious, long-term condition that significantly impacts individuals, families, and societies worldwide, ranking among the top 10 causes of adult death. The prevalence of diabetes is projected to rise by 25 %, with 578 million people expected to be affected by 2030, and 700 million by 2045 [1]. Diabetes mellitus (DM), characterized by hyperglycemia due to insulin secretion or action abnormalities, reduces glucose transport to the liver, muscle, and fat cells [2,3]. Type 2 DM, accounting for 90 - 95 % of cases, results from defective insulin secretion and tissue resistance to insulin [4].

Acarbose, miglitol, and voglibose are among the commonly used drugs for type 2 DM that effectively lower blood glucose levels. They operate through an α-glucosidase inhibitor (AGI) mechanism [5-7]. α-Glucosidase (EC 3.2.1.20) is a carbohydrate hydrolase that is widely present on the brush border of the small

intestinal mucosa and plays a crucial role in glycosyl structure. It is capable of hydrolyzing glycosidic bonds in various sugar compounds through either endonucleolytic or exonucleolytic processes, resulting in the formation of monosaccharides, oligosaccharides, or glycosaminoglycans, which contribute to increased postprandial blood glucose levels [8,9].

Inhibiting α-glucosidase activity slows carbohydrate digestion, which decreases glucose absorption into the bloodstream and helps regulate blood sugar levels. This inhibition is regarded as an important clinical target for the treatment of non-insulin-dependent diabetes mellitus [10,11]. In any case, right now accessible AGI drugs cause undesirable side impacts such as diarrhea, stomach pain, distension, and flatulence [12,13]. Hence, developing new AGI drugs with lower side impacts than synthetic ones is required, one of which is using medicinal plants with enzymatic activities, such as α-glucosidase inhibitors [14].

Syzygium cumini (L.) Skeels., a plant from the Myrtaceae family native to Asia, including Indonesia, has been proven to lower blood glucose levels. Its antidiabetic properties are recognized in traditional systems like Ayurveda, Unani, and Traditional Chinese Medicine (TCM) [15]. Leaves, seeds, and stem bark are commonly used for this purpose [16-18]. Active compounds in the leaves, such as myricetin, morin, quercetin, and bruceine A, have shown antidiabetic activity [19,20]. Java plum (*Syzygium cumini* var. *album*) is a variety whose existence is becoming increasingly rare and is classified under a specific conservation category [21]. Our previous study revealed that 8 flavonoid compounds from *S. cumini* var. *album* showed greater activity against target receptors compared to the positive control, acarbose. All flavonoids identified from *S. cumini* var. *album* exhibited superior activity against the target receptor, with D-(+)-catechin showing the highest affinity for α-glucosidase (ΔG = –5.94 kcal/mol; Ki = 44,270 nM) [7].

Although research on the activity of flavonoid compounds against type 2 DM has been conducted, specific studies on the ability of isolated active compounds to inhibit the α-glucosidase enzyme have not yet been carried out. Based on the references above, this study focuses on the isolation and identification of active compounds from leaves using a bioassay-guided isolation approach, targeting the inhibition of the α-glucosidase enzyme. The isolation of active compounds was performed using column chromatography, with the final stage carried out through radial chromatography. Additionally, the study evaluated the inhibitory activity of the active isolates against α-glucosidase both *in vitro* and *in silico*.

Materials and methods

Sample collection

The leaves and stem bark of *S. cumini* var. *album* were collected from Surabaya, East Java, Indonesia. The plant samples were taxonomically identified by a certified expert at Materia Medica Indonesia in Batu, East Java, Indonesia (No. 074/636/102-20-A/2022). The samples were cleaned by washing with clean water and then dried in an oven at approximately 50 °C, resulting in dried cimplicia material, which was subsequently ground to a particle size of 80 mesh for the extraction process.

Chemicals

p-Nitrophenyl-α-D-glucopyranoside (Sigma-Aldrich, Cat. No. N1377), Tris HCl buffer solution (Sigma-Aldrich, Cat. No. T3253), α-glucosidase from *Saccharomyces cerevisiae* (Sigma-Aldrich, Cat. No. G5003), acarbose 95 % (Sigma-Aldrich, Cat. No. A8980), and dimethyl sulfoxide (DMSO) (Merck, Germany) were used. The solvents used in the partitioning and purification steps included methanol (MeOH), both technical and pharmaceutical grades), Milli-Q (deionized) water, ethanol, n-butanol, ethyl acetate, and n-hexane.

Extraction and isolation

The leaves and stem bark of *S. cumini* var. *album* were each macerated with 70 % ethanol (1:10 w/v) in 3 separate repetitions, followed by solvent evaporation. The concentrated extract was then fractionated using liquid-liquid extraction with n-hexane, ethyl acetate, butanol, and water, respectively. The separation of the leaf extract was performed on the ethyl acetate fraction, following a method adapted from a previously established protocol [7], and further purified through radial chromatography [22]. Each step, from extraction to obtaining the active compound, was guided by the measurement of α-glucosidase inhibitors in a bioassay-guided isolation approach.

Compound identification

The spectrophotometer instruments used in this research included an Agilent NMR, operating at 500 MHz for ^{1}H and 125 MHz for ^{13}C. Quantitative analyses were conducted using UPLC with an XEVO TQD (Waters) system, equipped with an RP-18 ACQUITY Premier Column (100×2.1 mm, 1.7 μm).

α-glucosidase inhibitory assay

This study previously modified the α-glucosidase assay method using 96-well microplates [7,23]. Test samples at varying concentrations (10, 25, 50, 75 and 100 μg/mL) were mixed with 40 μL of 0.2 M phosphate buffer (pH 7.0) and 25 μL of 4-p-nitrophenyl α-D-glucopyranoside substrate. The mixture was incubated at 37 °C for 10 min, after which 25 μL of α-glucosidase solution (0.05 units/mL) was added and incubated again at 37 °C for an additional 15 min. The reaction was stopped by adding 100 μL of 0.2 M sodium carbonate solution [24,25]. The enzymatic hydrolysis of the substrate was measured using a Multiscan (ZN-320, ZN-390 plus) at 410 nm by quantifying the amount of p-nitrophenol released. For negative controls, α-glucosidase solution (0.05 units/mL), 20 mM 4-nitrophenyl β-D-glucopyranoside substrate, and 0.2 M phosphate buffer (pH 7.0) without any inhibitor were used. Acarbose was employed as the positive control in the experiment [26]. All experiments were performed in triplicate. The percentage of α-glucosidase inhibition was calculated using the following formula.

$$\%_{inhibition} = \frac{(A-C)-(B-C)}{(A-C)} \times 100\ \%$$

Information:

A = absorbance of negative control, B = absorbance of inhibitor with enzyme, C = absorbance of inhibitor without enzyme.

The IC_{50} value was calculated using a polynomial regression curve [23]. The concentration of the extract that inhibits α-glucosidase activity by 50 % can be determined using this equation.

Molecular docking analysis

The structure of the α-glucosidase target receptor (PDB ID: 3W37) was obtained from the Protein Data Bank (https://www.rcsb.org/). This structure includes acarbose as the native ligand bound to the enzyme. Molecular docking was conducted using AutoDockTools 4.2.6, with validation protocols as reported in previous studies [27,28], validation results were assessed using the Root Mean Square Deviation (RMSD) value. The process began with the validation step, utilizing a redocking strategy where the extracted co-crystal ligand from the receptor was used as the test ligand, and the co-crystal ligand's location was set as the binding site. The grid box was centered with dimensions of 32×50×26 $Å^3$, and the binding site coordinates for the α-glucosidase receptor were defined as x = 0.305, y = –1.705 and z = –23.114, with a grid spacing of 0.375 Å. AutoDockTools 4.2.6 was used for docking simulations under the following parameters: 27,000 genetic algorithm generations, 2,500,000 energy evaluations (Medium setting), a population size of 150 and 10 runs of the genetic algorithm (GA). Protein-ligand interactions were analyzed and visualized using BIOVIA Discovery Studio Visualizer v.21.1.0.20298.

Results and discussion

***In vitro* study of test samples against α-glucosidase inhibition**

The *in vitro* activity assessment of *S. cumini* var. *album* extracts, fractions, and rutin on the inhibition of α-glucosidase is presented in **Table 1**, all test treatment groups had significant differences with acarbose ($p < 0.005$).

Table 1 Inhibitory activity of *S. cumini* extracts, fractions, and rutin toward α-glucosidase.

Samples	IC_{50} ± SD (µg/mL)
70 % ethanol extract of *S. cumini* var. *album* leaves	96.96 ± 0.72*
70 % ethanol extract of *S. cumini* var. *album* stem bark	104.94 ± 0.66*
Ethyl acetate fraction of *S. cumini* var. *album* leaves	53.14 ± 0.41*
Butanol fraction of *S. cumini* var. *album* leaves	57.18 ± 0.16*
Water fraction of *S. cumini* var. *album* leaves	58.20 ± 0.21*
n-hexane fraction of *S. cumini* var. *album* leaves	54.53 ± 0.23*
Rutin	48.36 ± 0.4*
Acarbose	45.84 ± 0.27

NB: *: Sig. with acarbose ($p < 0.005$)

Identification of compounds

Structure elucidation

Spectrum data of ^{1}H-NMR and ^{13}C-NMR rutin are presented in **Table 2**.

Table 2 ^{1}H-NMR and ^{13}C-NMR spectroscope data (δ values) for rutin.

No. C	δC (ppm)	δH (∑H, m, J in Hz)	COSY	HMBC
2	156.49	-	-	-
3	133.15	-	-	-
4	177.24	-	-	-
5	161.09	-	-	-
6	98.54	6.20 (1H, d, J = 2.05 Hz)	H-8	C-5, C-7, C-8, C-10
7	163.93	-	-	-
8	93.46	6.39 (1H, d, J = 2.05 Hz)	H-6	C-6, C-7, C-9, C-10
9	156.29	-	-	-
10	103.83	-	-	-
1'	121.03	-	-	-
2'	116.13	7.53 (1H, s)	H-5'	C-2, C-3', C-4', C-6'
3'	144.62	-	-	-
4'	148.28	-	-	-
5'	115.09	6.84 (1H, d, J = 8.10 Hz)	H-2', H-6'	C-1', C-3', C-4'
6'	121.46	7.54 (1H, dd, J = 8.05 & 2.25 Hz)	H-5'	C-2, C-2', C-4'
OH-3'	-	9.20 (1H, s)	-	C-2', C-3', C-4'
OH-4'	-	9.69 (1H, s)	-	C-3', C-4', C-5'
OH-7	-	10.85 (1H, s)	-	C-6, C-7, C-8
OH-5	-	12.61 (1H, s)	-	-
		β-glucose		
1"	101.03	5.35 (1H, d, J = 7.30 Hz)	H-2"/H-5"	C-3
2"	76.28	3.21 (1H, m)	H-1"	C-1"
3"	75.76	3.23 (1H, m)	-	C-1"

No. C	δC (ppm)	δH (∑H, m, J in Hz)	COSY	HMBC
4"	69.85	3.06 (1H, m)	-	-
5"	73.93	3.21 (1H, m)	H-1", H-6"	C-1", C-6"
6"	66.87	3.71 (2H, d, J = 10.05 Hz)	H-5"	C-1'"
OH sugar glucose		5.10 (1H, d, J = 5.80 Hz)		
OH sugar glucose		5.14 (1H, d, J = 3.95 Hz)		
OH sugar glucose		5.31 (1H, d, J = 3.90 Hz)		C-1"
		α-rhamnose		
1'"	100.63	4.38 (1H, s)	H-3'"	-
2'"	70.41	3.27 (1H, m)	-	C-1'"
3'"	70.24	3.40 (1H, m)	H-1'"	C-1'"
4'"	71.69	3.08 (1H, m)	H-6'"	C-6'"
5'"	68.13	3.29 (1H, m)	H-6'"	C-1'"
6'"	17.63	1.00 (3H, d, J = 6.25 Hz)	H-4'", H-5'"	C-4'", C-5'"
OH sugar rhamnose		4.37 (1H, d, J = 5.00 Hz)		C-1'"
OH sugar rhamnose		4.43 (1H, d, J = 5.75 Hz)		
OH sugar rhamnose		4.56 (1H, d, J = 5.45 Hz)		

^{1}H-NMR; (500 MHz, (CD3)2CO): 6.20 (1H, d, J = 2.05 Hz, 6-CH); 6.39 (1H, d, J = 2.05 Hz, 8-CH); 7.53 (1H, s, 2'-CH); 6.84 (1H, d, J = 8.10 Hz, 5'-CH); 7.54 (1H, dd, J = 8.05 & 2.25 Hz, 6'-CH); 9.20 (1H, s,); 9.69 (1H, s); 10.85 (1H, s); 12.61 (1H, s); 5.35 (1H, d, J = 7.30 Hz, 1'-CH); 3.21 (1H, m, 2'-CH); 3.23 (1H, m, 3'-CH); 3.06 (1H, m, 4'-CH); 3.21 (1H, m, 5'-CH); 3.71 (2H, d, J = 10.05 Hz, 6'-CH2); 5.10 (1H, d, J = 5.80 Hz, OH glucose sugar); 5.14 (1H, d, J = 3.95 Hz, OH glucose sugar); 5.31 (1H, d, J = 3.90 Hz, OH glucose sugar); 4.38 (1H, s, 1'"-CH); 3.27 (1H, m, 2'"-CH); 3.40 (1H, m,3'"-CH); 3.08 (1H, m,4'"-CH); 3.29 (1H, m,5'"-CH); 1.00 (3H, d, J = 6.25 Hz, 6'"-CH3); 4.37 (1H, d, J = 5.00 Hz, OH rhamnose sugar); 4.43 (1H, d, J = 5.75 Hz, OH rhamnose sugar); 4.56 (1H, d, J=5.45 Hz, OH rhamnose sugar).
^{13}C-NMR; (125 MHz, (CD3)2CO): 156.49,2-C; 133.15,3-C; 177.24,4-C; 161.09,5-C; 98.54,6-CH; 163.93,7-C; 93.46,8-CH; 156.29,9-C; 103.83,10-C; 121.03,1'-C; 116.13,2'-CH; 144.62,3'-,C; 148.28,4'-C; 115.09,5'-CH; 121.46,6'-CH; 101.03,1"-CH; 76.28,2"-CH; 75.76,3"-CH; 69.85,4"-CH; 73.93,5"-CH; 66.87,6"-CH2; 100.63,1"-CH; 70.41,2"-CH; 70.24,3"-CH; 71.69,4"-CH; 68.13,5"-CH; 17.63,6"-CH3.

The ^{1}H-NMR data (**Figure 1**) showed that isolate 1 has peaks in both the aromatic and aliphatic regions, as well as several hydroxyl groups. The peak in the aromatic region (δH 6 - 8 ppm) consists of 5 protons, exhibiting a multiplicity pattern that indicates the presence of 2 different benzene rings. Two protons from the 1st ring (the flavonoid A ring) are observed at δH 6.20 (d) (H-6) and 6.39 (d) (H-8), which have a mutual meta relationship. The other 3 protons from the 2nd ring (the flavonoid B ring) appear at δH 6.84 (d) (H-5'), 7.53 (s) (H-2'), and 7.54 (dd) (H-6'), forming an ABX pattern where AB is ortho to each other (H-6' and H-5') and AX is meta (H-6' and H-2'). This aromatic proton pattern is typical for flavonoids and is supported by the presence of several singlet peaks at highly deshielded chemical shifts derived from the hydroxyl groups of the flavonoid ring at δH 9.20 (OH-3'), 9.69 (OH-4'), 10.85 (OH-7), and 12.61 (OH-5) [29-31].

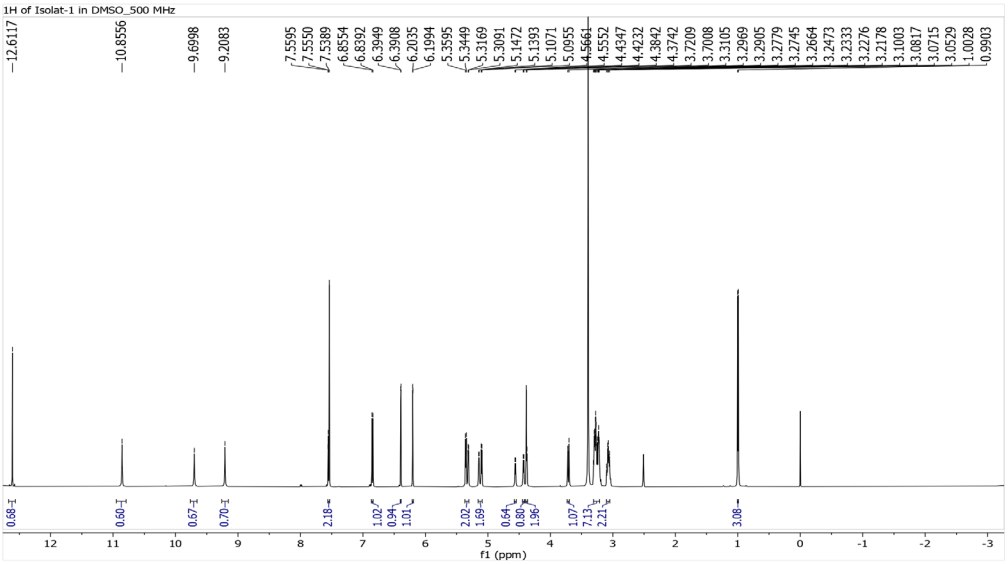

Figure 1 [1]H-NMR Spectra of isolate.

In the aliphatic region, protons also exhibit a typical pattern for sugar (hexose), with peaks accumulating between 3 - 4 ppm due to alkoxy protons, supported by peaks between 4 - 5 ppm, which are derived from hydroxyl (OH) groups in the sugar. Two highly deshielded methine protons exist at δH 5.35 (H-1" from β-glucose sugar) and 4.38 (H-1"' from α-rhamnose sugar). Additionally, there is one methylenedioxy proton at δH 3.71 (H-6" of sugar β-glucose) and only one methyl proton at δH 1.00 (H-6"' of sugar α-rhamnose), indicating the presence of 2 sugar groups bonded together to form disaccharide sugars of β-glucose and α-rhamnose [29-31].

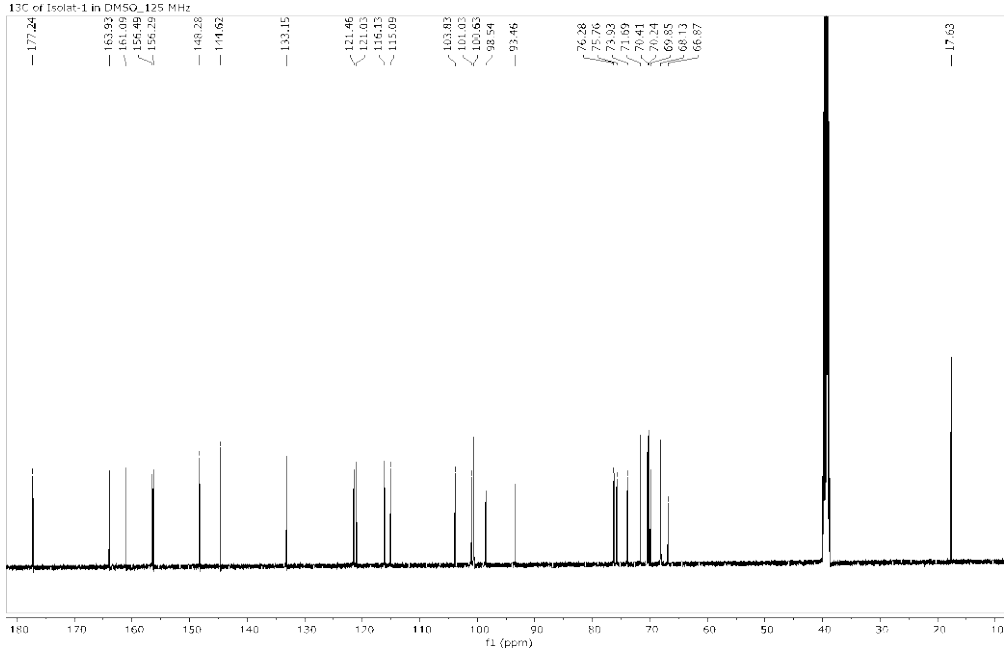

Figure 2 13C-NMR Spectra of isolate.

Based on the 13C-NMR data from isolate 1 (**Figure 2**), the compound exhibits carbonyl, aromatic, and aliphatic groups. The presence of 14 aromatic carbons and one carbonyl carbon is characteristic of the flavonoid skeleton, where the 14 aromatic carbons consist of 5 methine carbons and 9 quaternary carbons.

This aromatic skeleton is divided into 3 rings: ring A with 2 methines at δC 98.54 (C-6) and 93.46 (C-8), ring B with 3 methines at δC 115.09 (C-5'), 116.13 (C-2'), and 121.46 (C-6'), and ring C with one carbonyl at δC 177.24 (C-4). Seven of the 9 sp^2 quaternary carbons are oxyaryl carbons at δC 133.15 (C-3), 144.62 (C-3'), 148.28 (C-4'), 156.29 (C-9), 156.49 (C-2), 161.09 (C-5), and 163.93 (C-7) [29,31], with 4 of them bound to hydroxyl groups, supporting the classification of the compound as a flavonoid.

The aliphatic region consists of peaks at chemical shifts of 50 - 90 ppm, indicating the presence of oxygen-bound carbons in the sugar. There are 2 highly deshielded carbons at δC 101.03 (C-1" from sugar β-glucose) and 100.63 (C-1'" from sugar α-rhamnose), which are sp^3 carbons bound to 2 oxygen atoms. Additionally, there are 9 alkoxy carbons and one methyl carbon at δC 17.63 (C-6'" from sugar α-rhamnose), indicating the presence of 2 sugar groups that form a disaccharide. Based on the proton and carbon NMR data, it can be concluded that isolate 1 corresponds to the glycosidic flavonoid rutin, with the aglycone portion being quercetin and the glycone comprising a disaccharide sugar made up of β-glucose and α-rhamnose [29,31].

HMBC data demonstrate the correlation between protons and surrounding carbons, aiding in the assembly of the structure based on the ^{1}D-NMR readings (^{1}H and ^{13}C). The 1D-NMR data indicate that isolate 1 has a fundamental framework of glycosidized flavonoids. In the flavonoid aglycone section, correlations illustrate the relationships between each ring. In ring A, there is a correlation from protons 6.20 (d) (H-6) and 6.39 (d) (H-8) to the same carbon, 103.83 (C-10), and subsequently to 2 oxyaryl carbons that bind hydroxyl groups, 161.09 (C-5) and 163.93 (C-7). The distinction between positions 6 and 8 is made by the correlation of proton 6.20 (d) (H-6) to carbon 161.09 (C-5) and proton 6.39 (d) (H-8) to carbon 156.29 (C-9) [29-31].

Meanwhile, in ring B, correlations are observed from protons 6.84 (d) (H-5'), 7.53 (s) (H-2'), and 7.54 (dd) (H-6') to the same carbon, specifically 148.28 (C-4'), and then to 2 hydroxy-binding oxyaryl carbons, namely 144.62 (C-3') and 148.28 (C-4'). In ring C, the aliphatic sugar proton 5.35 (H-1" of β-glucose sugar) is correlated with carbon 133.15 (C-3), indicating that β-glucose sugar is directly bound to ring C of the flavonoids. The proton 3.71 (H-6" of β-glucose sugar) correlates with carbon 100.63 (C-1'" of α-rhamnose sugar), indicating the presence of 2 bonded sugar groups forming a disaccharide. The hydroxyl protons of each sugar ring are in adjacent regions, where one of the more deshielded protons, 5.31, correlates with carbon 101.03 (C-1") from sugar β-glucose, while the more shielded proton 4.37 correlates with carbon 100.63 (C-1'") from sugar α-rhamnose [29-31].

This HMBC data is corroborated by COSY data, which shows the correlation between protons that are neighbors or several bonds away. In the flavonoid aglycone skeleton, correlations are observed between H-6 and H-8 from ring A, and between H-2, H-5, and H-6 from ring B. In the β-glucose sugar skeleton, correlations are noted between H-1", H-2", and H-5". In the α-rhamnose sugar skeleton, correlations exist between H-1'" and H-3'", H-4'", H-5'", and H-6'" [29-31]. The overall structure can be seen in **Figure 3**.

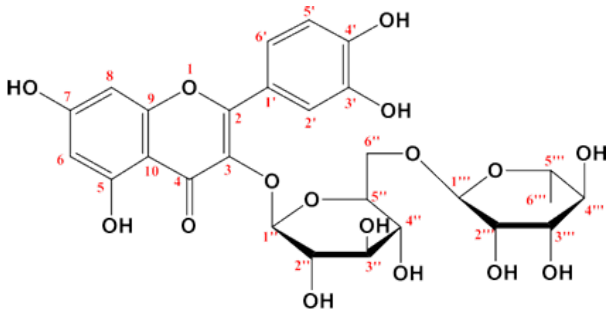

Figure 3 Rutin structure.

***In silico* study results**

The RMSD value of 1.72 Å indicates successful docking validation, as an RMSD value below 2 Å confirms the accuracy of the docking protocol [32,33].

Based on the docking results, rutin exhibited a less negative ΔG compared to acarbose. Since a more negative ΔG value signifies a stronger interaction between the ligand and the receptor, acarbose forms a more stable complex with the α-glucosidase receptor than rutin. The 2D and 3D visualizations of these interactions are presented in **Table 3**.

Table 3 The results of docking validation.

Compound	ΔG (kcal/mol)
Acarbose	–3.72
Rutin	–3.17

The active pocket of the α-glucosidase enzyme includes key amino acid residues located at positions 232 - 237 within the N-terminal N-loop. These residues are critical for the enzyme's biological activity, contributing to substrate binding and catalysis, thereby influencing the overall function of α-glucosidase. The re-docking of acarbose to α-glucosidase, crystallized by Tagami *et al.* [34] and Satoh *et al.* [35] from beet plants, showed the formation of 4 hydrogen bonds with residues Asp232, Asp357, Asp469, Asp568, and the formation of 4 hydrophobic bonds in the form of alkyl or pi-alkyl interaction with Trp432, Trp329, Ala234, and Phe236 [34,35]. Rutin binds to α-glucosidase by forming hydrogen bonds with the amino acid residues Asp232, Asp568, Met470, Arg562, Asp469, and Asp357. Additionally, it engages in 3 hydrophobic interactions with Trp329, Phe601, and Trp432, as shown in **Figure 5** and **Table 4**.

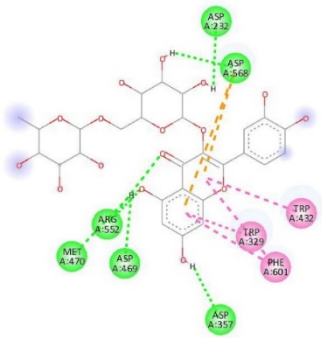

(A)

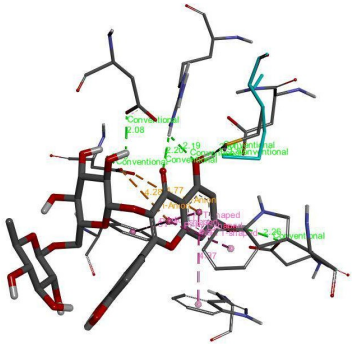

(A)

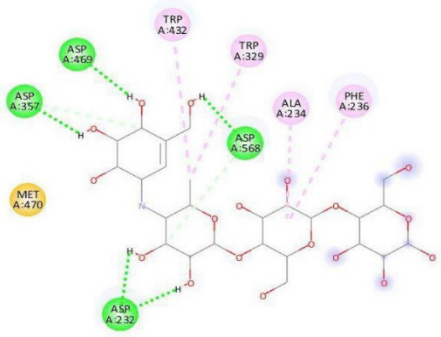

(B)

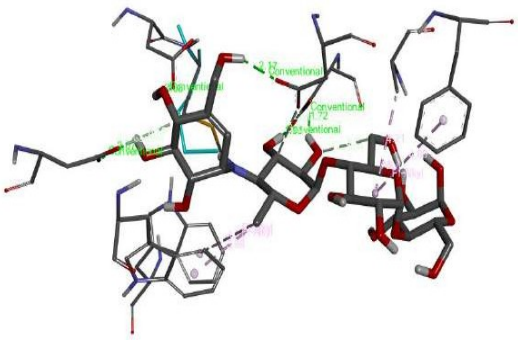

(B)

Figure 5 Interaction compounds with α-glucosidase; (A) Rutin, (B) Acarbose, (1) 2D, (2) 3D.

Table 4 Interaction of ligands and amino acid residues.

Code	Acarbose	Rutin
Glu29	2.99 Å	-
Asp232	-	2.08 Å
Asp303	1.90 Å	-
Trp329	-	✓
Asp357	-	2.26 Å
Trp415	✓	-
Trp432	-	✓
Asp443	2.35 Å	-
Asp469	-	1.83 Å
Met470	-	2.81 Å
Trp517	✓	-
Arg552	-	2.20 Å
Asp556	✓	-
Asp568	-	1.99 Å
Arg617	1.52 Å	-
Asp633	✓	-
Phe601	-	✓
Phe666	✓	-
Phe667	✓	-
His691	1.52 Å	-

NB: The hydrogen bond distance is given, and the hydrophobic and electrostatics interactions are indicated by a tick (✓).

Physicochemical properties influence biological activity. One of the physicochemical parameters affecting the biological activity of chemical compounds is electronic parameters, such as lowest unoccupied molecular orbital (E_{LUMO}) and highest occupied molecular orbital (E_{HOMO}). Increasing electronic properties is intended to play a role in drug interactions with receptors because it affects the ionization and polarization of drug compounds, resulting in increased pharmacological effects. E_{HOMO} shows the ability of a molecule to donate electrons to acceptors with empty molecular orbitals. Meanwhile, E_{LUMO} describes a molecule's ability to accept electrons. Molecules with high E_{HOMO} values have a high ability to donate electrons and tend to be more reactive. Additionally, molecules with low E_{LUMO} values have excellent electron acceptability compared to molecules with higher E_{LUMO} values [36,37]. The electronic parameters were calculated using the Chem 3D computer program, with the results illustrated in **Table 5**.

Table 5 Molecular orbital prediction results (Huckel calculations).

Compound	Molecular orbital (Huckel calculations)	E_{HOMO}	E_{LUMO}
Acarbose	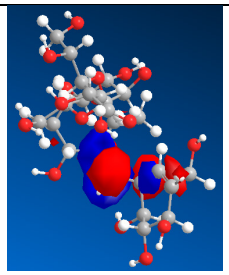	–9.674 eV	–3.166 eV
Rutin	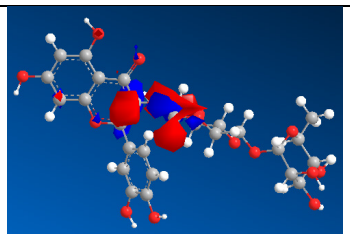	–10.354 eV	–4.787 eV

Results and discussion

This study revealed that rutin, a type of quercetin glycoside, is abundantly present in the ethyl acetate fraction of *S. cumini* var. *album* leaves, as confirmed by mass spectrometry, ^{1}H-NMR, and ^{13}C-NMR. Rutin is a key flavonoid that plays a crucial role in protecting plants from ultraviolet radiation and pathogens. In addition to its role in plant defense, rutin offers significant health benefits for humans, including the prevention of side effects associated with cancer treatment and the management of conditions such as hypercholesterolemia and diabetes mellitus. Its antioxidant and anti-inflammatory properties contribute to its therapeutic potential [38,39]. The presence of rutin has been reported in many plant species, including *S. cumini*, where 2.8 % of the rutin content is found in the leaf tissue [34]. Typically, leaves and flowers contain higher concentrations of phenolic acids and terpenoids compared to stems and roots [35,40].

Acarbose is considered safe and well tolerated, with a low occurrence of gastrointestinal side effects. It is widely accepted for diabetes treatment among Chinese patients and is a strong option for initial therapy in those newly diagnosed with type 2 DM [41]. Acarbose, a known α-glucosidase inhibitor, interacts with 8 amino acid residues Asp232, Asp357, Asp469, Asp568, Trp432, Trp329, Ala234, and Phe236 to inhibit the hydrolysis of polysaccharides into glucose (**Table 3**). The molecular docking study shows that rutin interacts with α-glucosidase through similar residues as acarbose, suggesting that rutin may also inhibit α-glucosidase. Another study identified acarbose as an α-glucosidase inhibitor, interacting with 7 residues Asp232, Ala234, Asn237, Asp357, Arg552, Asp568, and His626 by forming 14 hydrogen bonds within the active site of the N-loop. If an interaction occurs at the N-terminal position of the N-loop, it will inhibit the polysaccharide hydrolysis process into glucose [42]. Inhibition of α-glucosidase prevents the breakdown of carbohydrates in the digestive tract, ultimately reducing blood glucose levels [43]. This pharmacological activity is thought to be attributed to the presence of a double bond conjugated with a carbonyl group [34,44], as seen in the chemical structure of rutin (**Figure 3**).

When comparing the α-glucosidase inhibitory activity of different parts of *S. cumini* var. *album*, the leaves exhibited the highest activity, surpassing the bark (**Table 1**). The ethyl acetate fraction produced the lowest IC_{50} value at 53.14 µg/mL, compared to the n-hexane, butanol, and water fractions. The isolated rutin demonstrated an IC_{50} value of 48.36 µg/mL in inhibiting α-glucosidase, which was slightly higher than acarbose (IC_{50} = 45.84 µg/mL). Therefore, rutin shows great potential as an alternative antidiabetic drug, as its IC_{50} value is close to that of acarbose.

Previous studies have shown that secondary metabolites from *S. cumini* can inhibit α-glucosidase activity, particularly flavonoids [15,45-47]. Inhibition of α-glucosidase activity by various flavonoids, such as rutin, luteolin, myricetin, and quercetin, has also been

well documented in the literature [48-50]. Thus, the α-glucosidase inhibitory activity exhibited by *S. cumini* can largely be attributed to the phytochemical compounds it contains. Most α-glucosidase inhibitors function by mimicking the transition state of the pyranosidic unit of the natural glucosidase substrate, suggesting a likely competitive inhibition mechanism [51].

Conclusions

Rutin was isolated from the leaves of *S. cumini* var. *album* using a bioassay-guided approach. The compound was separated through gravity column chromatography and radial chromatography. Docking results indicated that rutin exhibited a more negative ΔG compared to acarbose. These binding interactions are similar to those of acarbose, a known α-glucosidase inhibitor. Rutin inhibited α-glucosidase (IC_{50} for rutin = 48.36 μg/mL; IC_{50} for acarbose = 45.84 μg/mL). Overall, rutin isolated from the leaves of *S. cumini* var. *album* shows potential for further development as an antidiabetic drug through its mechanism of α-glucosidase enzyme inhibition. This highlights the potential for rutin to be further explored and developed for future applications.

Acknowledgements

This research was funded by the Directorate General of Higher Education, Research, and Technology of the Ministry of Education, Culture, Research, and Technology through the Doctoral Research Scheme Program, under Contract Number 085/E5/PG.02.00.PT/2022.

References

[1] P Saeedi, I Petersohn, P Salpea, B Malanda, S Karuranga, N Unwin, S Colagiuri, L Guariguata, AA Motala, K Ogrtsova, JE Shaw, D Bright, R Williams and IDF Diabetes Atlas Committee. Global and regional diabetes prevalence estimates for 2019 and projections for 2030 and 2045: Results from the International Diabetes Federation Diabetes Atlas, 9th edition. *Diabetes Clinical Research* 2019; **157**, 107843.

[2] MZ Banday, AS Sameer and S Nissar. Pathophysiology of diabetes: An overview. *Avicenna Journal of Medicine* 2020; **10(4)**, 174-188.

[3] V Ormazabal, S Nair, O Elfeky, C Aguayo, C Salomon and FA Zuñiga. Association between insulin resistance and the development of cardiovascular disease. *Cardiovascular Diabetology* 2018; **17(1)**, 122.

[4] U Galicia-Garcia, A Benito-Vicente, S Jebari, A Larrea-Sebal, H Siddiqi, KB Uribe, H Ostolaza and C Martín. Pathophysiology of Type 2 diabetes mellitus. *International Journal of Molecular Sciences* 2020; **21(17)**, 6275.

[5] MIH Nayan, MM Alam, MA Jamil, JMA Hannan, I Haq and MI Hossain. An *in-vivo* study on postprandial hyperglycemia to assess antidiabetic activity of alcoholic extract of Cinnamomum verum bark. *Egyptian Pharmaceutical Journal* 2022; **21(2)**, 187-191.

[6] SV Moelands, PL Lucassen, RP Akkermans, WJD Grauw and FAVD Laar. Alpha-glucosidase inhibitors for prevention or delay of type 2 diabetes mellitus and its associated complications in people at increased risk of developing type 2 diabetes mellitus. *Cochrane Database of Systematic Reviews* 2018; **2018(12)**, CD005061.

[7] Y Andhiarto, Suciati, EN Praditapuspa and Sukardiman. *In silico* analysis and ADMET predicition of flavonoid compounds from Syzygium cumini var. *album* on α-glucosidase receptor for searching antidiabetic drug candidates. *Pharmacognosy Journal* 2022; **14(6)**, 736-743.

[8] GA Ismail, SF Gheda, AM Abo-Shady and OH Abdel-Karim. *In vitro* potential activity of some seaweeds as antioxidants and inhibitors of diabetic enzymes. *Journal of Food Science and Technology* 2019; **40(3)**, 681-691.

[9] M Attjioui, S Ryan, AK Ristic, T Higgins, O Goni, E Gibney, J Tierney and S O'Connell. Kinetics and mechanism of α-glucosidase inhibition by edible brown algae in the management of type 2 diabetes. *Proceedings of the Nutrition Society* 2020; **79(OCE2)**, E633.

[10] MA Syabana, ND Yuliana, I Batubara and D Fardiaz. Antidiabetic activity screening and nmr profile of vegetable and spices commonly

consumed in Indonesia. *Food Science and Technology* 2020; **41(1)**, 254-264.

[11] Y Feng, H Nan, H Zhou, P Xi and B Li. Mechanism of inhibition of α-glucosidase activity by bavachalcone. *Food Science and Technology* 2022; **42**, e123421.

[12] N Hamdy, M Abdel-Gabbar, HI Sakr, MA Abdelaziz, M Kandeil, AMA Aziz and OM Ahmed. Efficacy of metformin on different adipocytokines in type 2 diabetes mellitus patients. *Egyptian Pharmaceutical Journal* 2024; **23(2)**, 207-215.

[13] RJS Putra, A Achmad and H Rachma. Kejadian Efek Samping Potensial Terapi Obat Anti Diabetes Pasien Diabetes Melitus Berdasarkan Algoritma Naranjo. *Pharmaceutical Journal of Indonesia* 2017; **2(2)**, 45-50.

[14] AB Shah, S Yoon, JH Kim, K Zhumanova, YJ Ban, KW Lee and KH Park. Effectiveness of cyclohexyl functionality in ugonins from *Helminthostachys zeylanica* to PTP1B and α-glucosidase inhibitions. *International Journal of Biological Macromolecules* 2020; **165(Part B)**, 1822-1831.

[15] J Xiong, F Chen, J Zhang, W Ao, X Zhou, H Yang, Z Wu, L Wu, C Wang and Y Qiu. Occurrence of aflatoxin M1 in three types of milk from Xinjiang, China, and the risk of exposure for milk consumers in different age-sex groups. *Foods* 2022; **11(23)**, 3922.

[16] J Cao, C Chen, Y Wang, X Chen, Z Chen and X Luo. Influence of autologous dendritic cells on cytokine-induced killer cell proliferation, cell phenotype and antitumor activity *in vitro*. *Oncology Letters* 2016; **12(3)**, 2033-2037.

[17] H Xu, H Wang, W Zhao, S Fu, Y Li, W Ni, Y Xin, W Li, C Yang, Y Bai, M Zhan and L Lu. SUMO1 modification of methyltransferase-like 3 promotes tumor progression via regulating Snail mRNA homeostasis in hepatocellular carcinoma. *Theranostics* 2020; **10(13)**, 5671-5686.

[18] JM Li, X Li, LWC Chan, R Hu, T Zheng, H Li and S Yang. Lipotoxicity-polarised macrophage-derived exosomes regulate mitochondrial fitness through Miro1-mediated mitophagy inhibition and contribute to type 2 diabetes development in mice. *Diabetologia* 2023; **66(12)**, 2368-2386.

[19] RR Franco, LFR Zabisky, JPL Júnior, VHM Aves, A Justino, AL Saraiva, LR Goulart and FS Espindola. Antidiabetic effects of Syzygium cumini leaves: A non-hemolytic plant with potential against process of oxidation, glycation, inflammation and digestive enzymes catalysis. *Journal of Ethnopharmacology* 2020; **261(6)**, 113132.

[20] MR Alam, AB Rahma, M Moniruzzaman, MF Kadir, MA Haque, MRUH Alvi and M Ratan. Evaluation of antidiabetic phytochemicals in *Syzygium cumini* (L.) skeels (family: Myrtaceae). *Journal of Applied Pharmaceutical Science* 2012; **2(10)**, 94-98.

[21] A Khadivi, F Mirheidari, A Saeidifar and Y Moradi. Selection of the promising accessions of jamun (*Syzygium cumini* (L.) skeels) based on pomological characterizations. *Food Science & Nutrition* 2022; **11(1)**, 470-480.

[22] G Luo, Z Zhou, C Huang, P Zhang, N Sun, W Chen, C Deng, X Li, P Wu, J Tang and L Qing. Itaconic acid induces angiogenesis and suppresses apoptosis via Nrf2/autophagy to prolong the survival of multi-territory perforator flaps. *Heliyon* 2023; **9(7)**, e17909.

[23] N Putra, AN Garmana, NP Qomaladewi, Amrianto, LMR Al Muqarrabun, AR Rosandy, A Chahyadi, M Insanu and E Yaman. Bioactivity-guided isolation of a bioactive compound with α-glucosidase inhibitory activity from the leaves extract of Sauropus androgynous. *Sustainable Chemistry and Pharmacy* 2023; **31(1)**, 100907.

[24] MRF Pratama, H Poerwono and S Siswandono. Design and molecular docking of novel 5-O-Benzoylpinostrobin derivatives as anti-breast cancer. *Thai Journal of Pharmaceutical Sciences* 2019; **43(4)**, 201-212.

[25] MRF Pratama, H Poerwono and S Siswandono. Molecular docking of novel 5-O-benzoylpinostrobin derivatives as wild type and L858R/T790M/V948R mutant EGFR inhibitor. *Journal of Basic and Clinical Physiology and Pharmacology* 2019; **30(6)** 20190301.

[26] DL Aulifa, IK Adnyana, S Sukrasno and J Levita. Inhibitory activity of xanthoangelol isolated from Ashitaba (Angelica keiskei Koidzumi) towards α-

glucosidase and dipeptidyl peptidase-IV: *In silico* and *in vitro* studies. *Heliyon* 2022; 8(5), e09501.

[27] L Luo, R Wang, X Wang, Z Ma and N Li. Compounds from angelica keiskei with NQO1 induction, DPPH radical dot scavenging and α-glucosidase inhibitory activities. *Food Chemistry* 2012; **131(3)**, 992-998.

[28] Y Liu, X Zhou, D Zhou, Y Jian, J Jia and F Ge. Isolation of *Chalcomoracin* as a potential α-glycosidase inhibitor from mulberry leaves and its binding mechanism. *Molecules* 2022; **27(18)**, 5742.

[29] RH Bible. *Interpretation of NMR spectra: An empirical approach.* Springer Science & Business Media, New Jersey, 2013.

[30] T Parker, E Limer, AD Watson, M Defernez, D Williamson and EK Kemsley. 60 MHz 1H NMR spectroscopy for the analysis of edible oils. *Trends in Analytical Chemistry* 2014; **57(100)**, 147-158.

[31] R Gunawan and ABD Nandiyanto. How to read and interpret 1H-NMR and 13C-NMR spectrums. *Indonesian Journal of Science and Technology* 2021; **6(2)**, 267-298.

[32] FA Muslikh, RR Samudra, B Ma'arif, ZS Ulhaq, S Hardjono and M Agil. *In silico* molecular docking and ADMET analysis for drug development of phytoestrogens compound with its evaluation of neurodegenerative diseases. *Borneo Journal of Pharmacy* 2022; **5(4)**, 357-366.

[33] ME Gondokesumo, FA Muslikh, RR Pratama, B Ma'arif, D Aryantini, R Alrayan and D Luthfiana. The potential of 12 flavonoid compounds as alzheimer's inhibitors through an *in silico* approach. *Eurasian Chemical Communications* 2023; **6**, 50-61

[34] T Tagami, K Yamashita, M Okuyama, H Mori, M Yao and A Kimura. Molecular basis for the recognition of long-chain substrates by plant α-glucosidases. *Journal of Biological Chemistry* 2013; **288(26)**, 19296-19303.

[35] T Satoh, T Toshimori, G Yan, T Yamaguchi and K Kato. Structural basis for two-step glucose trimming by glucosidase II involved in ER glycoprotein quality control. *Scientific Reports* 2016; **6(1)**, 20575.

[36] I Redzepovic, B Furtula and I Gutman. Relating total π-electron energy of benzenoid hydrocarbons with HOMO and LOMO energies. *MATCH Communications in Mathematical and in Computer* 2020; **84(1)**, 229-237.

[37] AM Ghassab. Phytoconstituents of methanolic extract of fenugreek seeds as a green corrosion inhibitor of metals (Fe, Al and Cu). *Jordanian Journal of Engineering and Chemical Industries* 2021; **4(1)**, 24-33.

[38] Z Sheng, H Dai, S Pan, H Wang, Y Hu and W Ma. Isolation and characterization of an α-glucosidase inhibitor from Musa spp. (Baxijiao) flowers. *Molecules* 2014; **19(7)**, 10563-10573.

[39] R Agada, WA Usman, S Shehu and D Thagariki. *In vitro* and *in vivo* inhibitory effects of *Carica papaya* seed on α-amylase and α-glucosidase enzymes. *Heliyon* 2020; **6(3)**, e03618.

[40] Y Zhao, S Chen, F Shen, D Long, T Yu, M Wu and X Lin. *In vitro* neutralization of autocrine IL-10 affects Op18/stathmin signaling in non-small cell lung cancer cells. *Oncology Reports* 2019; **41(1)**, 501-511.

[41] K He, JC Shi and XM Mao. Safety and efficacy of acarbose in the treatment of diabetes in Chinese patients. *Therapeutics and Clinical Risk Management* 2014; **10**, 505-511.

[42] A Ganeshpurkar and AK Saluja. The pharmacological potential of rutin. *Saudi Pharmaceutical Journal* 2017; **25(2)**, 149-164.

[43] YJ Sun, JM He and JQ Kong. Characterization of two flavonol synthases with iron-independent flavanone 3-hydroxylase activity from *Ornithogalum caudatum* Jacq. *BMC Plant Biology* 2019; **19(1)**, 195.

[44] LA Nogueira, YG Figueiredo, ALCC Ramos, VTDV Correia, BV Nunes, LV Ribeiro, AO Franco, RB Ferreira, I Sousa, J Mota, P Batitsta-Santos, RLBD Araujo and JOF Melo. The presence of flavonoids in some products and fruits of the genus *eugenia*: An integrative review. *Frontiers in Food Science and Technology* 2022; **2**, 899492.

[45] S Kamtekar, V Keer and V Patil. Estimation of phenolic content, flavonoid content, antioxidant and alpha amylase inhibitory activity of marketed polyherbal formulation. *Journal of Applied Pharmaceutical Science* 2014; **4(09)**, 61-65.

[46] JJ DiNicolantonio, J Bhutani and JH O'Keefe. Acarbose: Safe and effective for lowering postprandial hyperglycaemia and improving cardiovascular outcomes. *Open Heart* 2015; **2(1)**, e000327.

[47] H Wang, H Li, Y Hou, P Zhang and M Tan. Plant polysaccharides: Sources, structures, and antidiabetic effects. *Current Opinion in Food Science* 2023; **51(2)**, 101013.

[48] S Govindan, J Shanmugam, G Rajendran, P Ramani, D Unni, B Venkatachalam, A Janardhanan, K Aswini, RL Rajendran, P Gangadaran and BC Ahn. Antidiabetic activity of polysaccharide from *Hypsizygus ulmarius* in streptozotocin-nicotinamide induced diabetic rats. *Bioactive Carbohydrates and Dietary Fibre* 2023; **29**, 100350.

[49] F Kianersi, MR Abdollahi, A Mirzaie-Asl, D Dastan and F Rasheed. Identification and tissue-specific expression of rutin biosynthetic pathway genes in *Capparis spinosa* elicited with salicylic acid and methyl jasmonate. *Scientific Reports* 2020; **10(1)**, 8884.

[50] E Barber, MJ Houghton and G Williamson. Flavonoids as human intestinal α-glucosidase inhibitors. *Foods* 2021; **10(8)**, 1939.

[51] MAT Phan, J Wang, J Tang, YZ Lee and K Ng. Evaluation of α-glucosidase inhibition potential of some flavonoids from *Epimedium brevicornum*. *LWT* 2013; **53(2)**, 492-498.